Monoenergetic electron parameters in a spheroid bubble model

H. Sattarian[a)†], Sh. Rahmatallahpur,[b)] and T. Tohidi[c)]

[a)] *Maraghe Branch, Physics Department, Islamic Azad University, Maragheh, Iran*
[b)] *Bonab Branch, Physics Department, Islamic Azad University, Bonab, Iran*
[c)] *Department of Physics, Azarbaijan University of Tarbiat Moallem, Tabriz, Iran*

(Received 11 May 2011; revised manuscript received 15 August 2012)

A reliable analytical expression for the potential of plasma waves with phase velocities near the speed of light is derived. The presented spheroid cavity model is more consistent than the previous spherical and ellipsoidal models and it explains the mono-energetic electron trajectory more accurately, especially at the relativistic region. The maximum energy of electrons is calculated and it is shown that the maximum energy of the spheroid model is less than that of the spherical model. The electron energy spectrum is also calculated and it is found that the energy distribution ratio of electrons $\Delta E/E$ for the spheroid model under the conditions reported here is half that of the spherical model and it is in good agreement with the experimental value in the same conditions. As a result, the quasi-mono-energetic electron output beam interacting with the laser plasma can be more appropriately described with this model.

Keywords: quasi-mono-energetic electron bunches, intense laser, plasma accelerator, laser wake field, bubble regime

PACS: 52.38.−r, 41.75.Jv, 42.62.−b, 41.75.Lx **DOI:** 10.1088/1674-1056/22/2/025203

1. Introduction

Currently, the production of electron beams with low energy spread, high energy, and low divergence by using short, intense laser pulses is very active. In plasma-based acceleration, a phase velocity close to the speed of light driven by an intense laser beam can be obtained. When an intense laser beam is used it is called laser wake-field acceleration (LWFA).[1–3]

One of the applications of the high intensity laser-plasma interaction is high gradient electron acceleration. The ponderomotive force of a relativistic intense laser pulse can push plasma electrons away from a high intensity region. This creates a plasma cavity, or bubble, that is devoid of plasma electrons. The resulting plasma bubble follows in the wake of the laser pulse propagating with the group velocity v_0. Strong longitudinal (E_x) and transverse electric fields inside the bubble are responsible for acceleration and focusing of the relativistic electrons which can, under the right circumstances, be injected into the bubble from the ambient plasma. The huge charge of unshielded ions provides strong accelerating and focusing fields inside the bubble. Moreover, a large number of background plasma electrons can be trapped in the bubble and accelerated up to high energies.

Different models of electron acceleration are considered and examined to achieve a mono-energetic electron and ion beam, among which the bubble regime is one of the most recent methods used in laser-plasma accelerators.[4–15] In the laser wake-field acceleration (LWFA) scheme enabled by a short laser pulse whose frequency (ω_0) is much larger than the plasma frequency (ω_p), the bubble is created due to the ponderomotive force. As an intense pulse propagates through an underdense plasma with $\omega_0 \gg \omega_p$, the ponderomotive force associated with the laser envelope expels electrons from the region of the laser pulse and excites highly nonlinear, relativistic electron plasma waves.

Although many experimental achievements have been reported, there are still large differences between the experimental measurements and theoretical calculations of parameters of a mono-energetic electron beam produced in the bubble regime. In the spherical model of Pukhov *et al.*,[16] which was an important step forward in the explanation of the bubble regime, the predicted maximum energy of mono-energetic electron bunches was more than two times that predicted by PIC simulation or experimentally measured. They have explained this obvious disagreement as a result of the spherical assumption of the bubble.[4,5] In fact, this was mentioned in the later works.[12,13]

With reproducible equations of the bubble regime, we showed that the equation of the potential in Pukhov *et al.* is limited to spherical bubbles, which do not accurately model the true shape expected, and better results can be obtained assuming an elliptical shape as is done in the present model. These reliable results correctly explain the effect of the elongation on the variation of mono-energetic electron energy spectrum at the relativistic region.

†Corresponding author. E-mail: hsattarian@yahoo.com; rahmatsh@yahoo.com

© 2013 Chinese Physical Society and IOP Publishing Ltd

2. The fields inside the spheroid cavity

In this work we improve the previous models and resolve the ambiguity in the shape of the potential by correcting equations in the previous spherical model[4,5] and the ellipsoidal model.[13,14]

The spherical models in Refs. [4] and [5] are incomplete due to different coefficients in Eqs. (11) and (12) where the coefficients in our Eq. (5) and Eq. (7) are corrected from 1/2 in Refs. [4] and [5] to 1 and a previously omitted equation is added (Eq. (6) presented in this paper).

The model in Refs. [13] and [14] starts with this equation

$$\ddot{r}\hat{r} = \frac{\mathrm{d}v}{\mathrm{d}t}\hat{r} = -\frac{1}{\mu}\left(e\nabla\Phi_i\hat{r} + E_p\hat{\theta}\right). \tag{1}$$

Moreover, by separating them into the radial and tangential components reach to

$$\hat{r} : (\ddot{r} - r\dot{\theta}^2)^{\hat{r}} = -\frac{e}{\mu}\frac{Q_i}{4\pi\varepsilon_0 r^2}\hat{r}, \tag{2a}$$

$$\hat{\theta} : \frac{1}{r}\frac{\mathrm{d}}{\mathrm{d}t}(r^2\dot{\theta})\hat{\theta} = \frac{E_p}{\mu}\hat{\theta}, \tag{2b}$$

where Φ_i, e, and θ are the potential of the cavity average ion charge, the electron charge, and the tangential component, respectively. Then we define system's constant angular momentum (ℓ) as $l = |E| = \mu r^2\dot{\theta}$ and finally reach $r(\theta) = \alpha/(1+\varepsilon\cos\theta)$. Here the trajectory forms hyperbola if $\varepsilon > 1$, parabola if $\varepsilon = 1$, ellipse if $0 < \varepsilon < 1$, and circle if $\varepsilon = 0$. The main defect of this model is assumptions on constancy of angular momentum (l). If (l) is constant we obviously see from Eq. (2b) that the ponderomotive force E_p, is zero and it disappears completely and the solution to central force of Eq. (2a) is an ellipsoid as in Ref. [16].

Therefore, in this section we derive the correct solution to Maxwell's equations. We solve the problem and derive a new model, which both complies with Maxwell's equations and particle in a cell (PIC) simulations and experimental measurements.

In this work, a mobile cavity, which contains relativistic electrons through immobile ions in the plasma, is considered. The cavity runs with the normalized relativistic velocity $v_0 = v/c \approx 1$ along x axis. The ion dynamics are neglected because the cavity dimensions are assumed to be smaller than the ion response length $\approx c/\omega_\mathrm{pi}$, where $\omega_\mathrm{pi} = (4\pi e^2 n_0/M)$ is the ion plasma frequency and M is the ion mass.

Starting from Maxwell's equations, we obtain

$$\Delta\varphi + \frac{\partial}{\partial t}\nabla\boldsymbol{A} = n - 1, \tag{3}$$

$$\Delta\boldsymbol{A} - \frac{\partial^2 A}{\partial t^2} - \nabla\left(\nabla\boldsymbol{A} + \frac{\partial\varphi}{\partial t}\right) = \frac{np}{\gamma}, \tag{4}$$

where φ is the scalar potential, $\boldsymbol{A}$ is the vector potential, n is the electron density inside the cavity, p is the momentum of the electrons and γ is the energy of electrons. By writing Maxwell's equations in terms of potentials and using a convenient gauge $A_x = -\varphi$, and using a quasi static approximation (QSA), assuming that all quantities depend on the parameter $\xi = x - v_0 t$ instead of x and t, where v_0 is the relativistic velocity of the cavity along the x axis, then we have

$$\Delta\Phi = -\left(\frac{2v_0^2}{1+v_0}\right)\frac{\partial}{\partial\xi}(\nabla_\perp\boldsymbol{A}_\perp) + \frac{2}{(1+v_0)^2}(1+v_0+v_0^2), \tag{5}$$

$$\Delta\Phi = v_0^2\frac{\partial^2}{\partial\xi^2}\Phi + \frac{2}{1+v_0}, \tag{6}$$

$$\Delta\boldsymbol{A}_\perp - v_0^2\frac{\partial^2}{\partial\xi^2}\boldsymbol{A}_\perp = \nabla_\perp\left(\frac{1+v_0}{2}\frac{\partial\Phi}{\partial\xi} + \nabla_\perp\boldsymbol{A}_\perp\right). \tag{7}$$

We have assumed that inside the cavity $(n = 0)$. Here we use the wake field potential of $\Phi = A_x - \varphi$ instead of the scalar one. We use dimensionless units, normalizing the time to ω_p^{-1}, the lengths to c/ω_p, the velocity to c, the electromagnetic fields to $mc\omega_\mathrm{p}/|e|$, and the electron density, n to the background density n_0.

In a complete spheroid model unlike the earlier mentioned works, equation (6) is also needed and the coefficients in Eqs. (5) and (7) should be corrected from 1/2 in Refs. [4] and [5] to 1.

In the following paragraph, we derive the correct solution to the above equations.

From Eqs. (5) and (6) we have

$$-\left(\frac{2v_0^2}{1+v_0}\right)\frac{\partial}{\partial\xi}(\nabla_\perp\boldsymbol{A}_\perp) + \frac{2}{(1+v_0)^2}(1+v_0+v_0^2) = v_0^2\frac{\partial^2}{\partial\xi^2}\Phi + \frac{2}{1+v_0}.$$

By rearranging the above equation we get

$$\nabla_\perp\boldsymbol{A}_\perp = -\frac{1+v_0}{2}\frac{\partial}{\partial\xi}\Phi + \frac{1}{1+v_0}\xi. \tag{8}$$

And by substituting Eq. (8) into Eq. (7) we have

$$\Delta\boldsymbol{A}_\perp - v_0^2\frac{\partial^2}{\partial\xi^2}\boldsymbol{A}_\perp = 0. \tag{9}$$

Moreover, from Eq. (6) we have

$$\Delta_\perp\Phi + (1-v_0^2)\frac{\partial^2}{\partial\xi^2}\Phi = \frac{2}{1+v_0},$$

where

$$\Delta_\perp\Phi = \frac{\partial^2}{\partial y^2}\Phi + \frac{\partial^2}{\partial z^2}\Phi,$$

or

$$\Delta_\perp\Phi = -(1-v_0^2)\frac{\partial^2}{\partial\xi^2}\Phi + \frac{2}{1+v_0}. \tag{10}$$

By assuming that potential Φ depends separately on ξ and y,z as $\Phi(\xi,y,z) = \phi 1(y,z) + f(\xi)$, we can separate Eq. (10) as

$$\Delta_\perp\Phi = \alpha(v_o), \tag{11}$$

$$-(1-v_0^2)\frac{\partial^2}{\partial\xi^2}\Phi + \frac{2}{1+v_0} = \alpha(v_0). \tag{12}$$

The constant α can be any parameter or depend on any other variable except the independent variables ξ, y, z, here we assume that the parameter α, which is just independent of ξ, y,

z can depend on v_0 as $\alpha(v_0)$. As seen from Eq. (12) if we let $v_0 = 1$ then α should be $\alpha(v_0) = 1$ and we reach to a null equation $0 = 0$ and the dependency of potential Φ on ξ component completely disappears. In this case, the solutions of Eq. (11) and Eq. (12) are as follows:

$$\Phi(\xi, y, z) = \frac{y^2}{4} + \frac{z^2}{4} + f(\xi), \tag{13}$$

where $f(\xi)$ is assumed to be any function. For $v_0 = 1$ and $\alpha(v_0) = 1$ the correct solution is Eq. (13). So we see that the solutions would be general with no idea of how Φ depends on ξ. Based on the correct derivation of a model from Maxwell's equations mentioned here (i.e., Eqs. (5), (6), and (7)), by assuming a nonrealistic $v_0 = 1$, it is impossible to reach mathematically to the potential

$$\Phi(\xi, y, z) = \frac{y^2}{4} + \frac{z^2}{4} + \frac{\xi^2}{4}$$

as in Refs. [4] and [5], unless assuming a symmetric and spherical Φ beforehand. Therefore, to reach to the solution

$$\Phi(\xi, y, z) = \frac{y^2}{4} + \frac{z^2}{4} + \frac{\xi^2}{4},$$

one assumes a spherical solution and in this case, one could choose $f(\xi) = \xi^2/4$ as in Refs. [4] and [5].

Although we can arbitrary reach in the limit to near $v_0 = 1$, we always have $v_0 < 1$, so in the solution we must consider this critical condition and derive the correct solution, which also agrees in the limit of $v_0 = 1$.

By starting from Eq. (12) we get

$$(1 - v_0^2)\frac{\partial^2}{\partial \xi^2} f(\xi) = \frac{2}{1 + v_0} - \alpha(v_0) \tag{14}$$

or

$$\begin{aligned} f(\xi) &= \frac{1}{1 - v_0^2}\left(\frac{2}{1 + v_0} - \alpha(v_0)\right)\frac{\xi^2}{2} \\ &= \frac{1}{1 - v_0^2}\left(\frac{2 - \alpha(v_0) - v_0\alpha(v_0)}{1 + v_0}\right)\frac{\xi^2}{2} \\ &= \frac{(\alpha(v_0) + 2\alpha'(v_0))\xi^2}{8}, \quad \alpha(1) = 1. \end{aligned} \tag{15}$$

Here we assumed that the constant α which is just independent of ξ, y, z, can depend on v_0 and to have a continuous potential, we let $v_0 \to 1$ in the limit and obtain the above solution for the ξ component of Φ and for brevity we let $\alpha' = [\mathrm{d}/(\mathrm{d}v_0)]\alpha(v_0)$ and $\alpha = \alpha(v_0)$.

And the solution of Eq. (11) in the limit is

$$\phi 1(y, z) = \frac{y^2}{4} + \frac{z^2}{4}$$

or

$$\Phi(\xi, y, z) = \phi 1(y, z) + f(\xi) = \frac{(1 + 2\alpha')\xi^2}{8} + \frac{y^2}{4} + \frac{z^2}{4} + \mathrm{con}.$$

The constant of integration con is chosen as $\mathrm{con} = 1 + \phi_0$ so that on the surface of spheroid $\Phi = 1$.

Considering Eq. (8) we have

$$\nabla_\perp A_\perp = \frac{1 - 2\alpha'}{4}\xi. \tag{16}$$

Based on the symmetry in y and z directions we can choose

$$\frac{\partial}{\partial y}A_y = \frac{\partial}{\partial z}A_z = \frac{1 - 2\alpha'}{8}\xi.$$

A solution satisfying Eq. (9) with the above condition is:

$$A_\perp = \left(\frac{1 - 2\alpha'}{8}y\xi,\ \frac{1 - 2\alpha'}{8}z\xi\right).$$

Therefore, we have

$$\Phi(\xi, y, z) = 1 + \left(\frac{(1 + 2\alpha')\xi^2}{8} + \frac{y^2}{4} + \frac{z^2}{4} - \phi_0\right), \tag{17}$$

$$A = (A_x, A_\perp) = \left(\frac{\Phi}{2},\ \frac{1 - 2\alpha'}{8}y\xi,\ \frac{1 - 2\alpha'}{8}z\xi\right). \tag{18}$$

In general as seen from Eq. (17) the coefficients of ξ, y are not equal and depend on the parameter $\alpha' = \alpha'(v_0)$. By defining the eccentricity as $\varepsilon = \sqrt{1 - (b^2/a^2)}$ where $a^2 = 8\phi_0/(1 + 2\alpha')$, $b^2 = 8\phi_0/2$, we get $\varepsilon = \sqrt{1 - 2\alpha'/2}$, the eccentricity of the spheroid depends on parameter α'. In the next section by choosing this parameter properly we can simulate the bubble regime more accurately.

3. The trajectory of the electrons

The energy of electrons in a spheroid cavity can be derived using the Hamiltonian formulation. The Hamiltonian of a charged particle in an electromagnetic field is

$$H = \sqrt{1 + (\boldsymbol{P}_\mathrm{c} + \boldsymbol{A})^2 + \boldsymbol{a}^2} - v_0\boldsymbol{P}_\mathrm{c} - \varphi, \tag{19}$$

where $\boldsymbol{P}_\mathrm{c}$ is the particle canonical momentum, $\boldsymbol{a}$ is normalized vector potential of the laser field, and φ is the scalar potential. The above Hamiltonian can be written as

$$H = \sqrt{1 + p^2 + a^2} - v_0 p + \Phi. \tag{20}$$

Here p is the momentum and we have used the wake potential Φ. The Hamiltonian can be split into two parts by expanding it in the power of p^2. The first part determines the longitudinal motion and the second part determines the transverse motion. We obtain the longitudinal Hamiltonian and consider only the x dimension

$$H_{||} = \sqrt{1 + p_x^2 + a^2} - v_0 p_x + \Phi(\xi, 0, 0). \tag{21}$$

Here p_x is x component of the momentum. With the assumption $p_x \gg \gamma_0$, and $a \approx 0$ and reformulating potential of Eq. (17) as

$$\begin{aligned} &\Phi(\xi, y, z) = 1 + \phi_0\left(\frac{\xi^2}{a^2} + \frac{y^2}{b^2} + \frac{z^2}{b^2} - 1\right), \\ &\frac{\phi_0}{a^2} = \frac{1 + 2\alpha'}{8}, \quad \frac{\phi_0}{b^2} = \frac{2}{8}. \end{aligned} \tag{22}$$

Therefore, the equation of motion is

$$-\dot{p}_x = \frac{\partial}{\partial \xi}H_{||} = 2\phi_0\frac{\xi}{a^2}, \quad \dot{\xi} = \frac{\partial}{\partial p_x}H_{||} = \frac{p_x}{\sqrt{1 + p_x^2}} - v_0. \tag{23}$$

From the transversal part of Eq. (20) we have

$$H_\perp = \frac{p_y}{2p_x^2} + \phi_0\frac{y^2}{b^2}. \tag{24}$$

The motions are then

$$\dot{y} = \frac{p_y}{p_x}, \quad \dot{p}_y = -\phi_0 \frac{y}{2b^2}. \tag{25}$$

Trajectories of two different electrons trapped and untrapped in the potential of spherical and spheroid models for the same initial momentums and position in the y and ξ phase spaces are shown in Fig. 1.

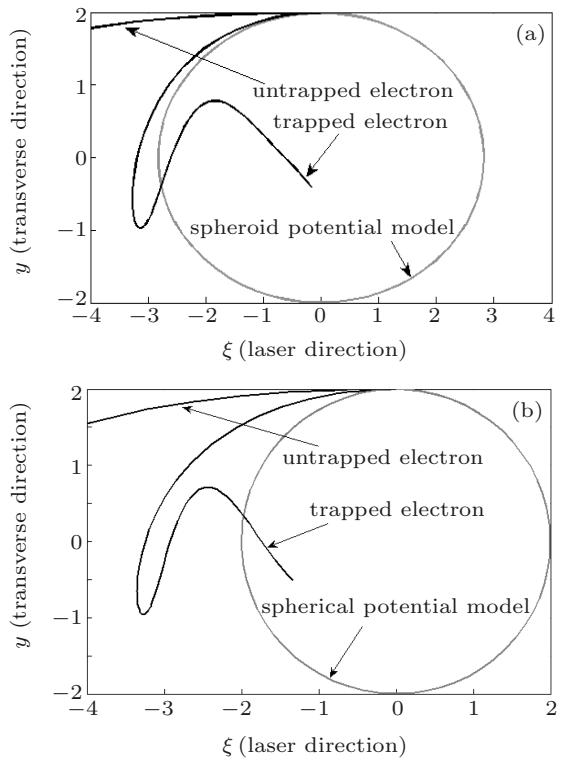


Fig. 1. Trajectory of two different electrons trapped and untrapped in the potential of spherical and spheroid models for the same initial momentums and position in the y and ξ phase spaces.

4. The energy of electrons

From Eq. (21) we can derive the following equation

$$H_{||} = \sqrt{1+p_x^2} - v_0 p_x + \Phi(\xi,0,0) \approx 2,$$

where the initial conditions of $p_x = a = 0$, $\Phi(\xi,0,0) = 1$ are applied. From the above equation and for $\gamma = \sqrt{1+p_x^2} \gg \gamma_0$ we have

$$\gamma = \sqrt{1+p_x^2} \approx 2\gamma_0^2(2-\Phi(\xi,0,0)$$
$$= 2\gamma_0^2\Big(1+\phi_0(1-\frac{\xi^2}{a^2})\Big) \approx 2\gamma_0^2\phi_0\Big(1-\frac{\xi^2}{a^2}\Big).$$

The maximum energy of the accelerated electrons peaked at the cavity center is

$$\gamma_{\max} \approx 2\gamma_0^2\phi_0 = \gamma_0^2\frac{(1+2\alpha')a^2}{4} = \gamma_0^2\frac{b^2}{2}. \tag{26}$$

In order to compare the spheroid model with the spherical one, let

$$\frac{\phi_0^{3/2}}{4\sqrt{2}} = ab^2 = R^3, \tag{27}$$

where R is the radius of a sphere, in this case spheroid and sphere have equal volume and equal charge density (here normalized to $n = 1$), if we let $a = b = R$ in Eq. (26), we have

$$\gamma_{\max\,\text{sphere}} \approx \gamma_0^2 R^2/2. \tag{28}$$

By comparing Eqs. (26)–(28) we can see that

$$\gamma_{\max} \le \gamma_{\max\,\text{spherical}}. \tag{29}$$

As a result, the maximum energy of the spheroid model is less than that of the spherical model, and it is closer to PIC simulations[4,5] than that in the spherical model.

The normalized energy spectrum of the electron bunch inside cavity can be obtained from Ref. [17] as

$$\frac{\mathrm{d}N}{\mathrm{d}E} = \frac{\sqrt{\gamma_{\max}-E}-\sqrt{\delta E-E}}{\gamma_{\max}^{3/2}-(\gamma_{\max}-\delta E)^{3/2}}, \tag{30}$$

where δE represents the initial energy spread of electrons before entering the bubble.

In Fig. 2, the results calculated from the introduced spheroid model are compared with experimental results and the spherical model. For comparison, we have assumed that the total area under curves $E_{\max} \times \Delta E$ of the elliptical and spherical models are equal with experimental data. According to Eq. (29) in as much as $\gamma_{\max} \le \gamma_{\max\,\text{spherical}}$, therefore, for the same area under the curve the peak in the spherical model should be less than the one in the spheroid. We plotted spherical and elliptical models for $\alpha = 1$, $\alpha' = 0$. As we can see, it is in good agreement between the experimental and spheroid results while the results predicted by the spherical model are further from the experimental measurements.

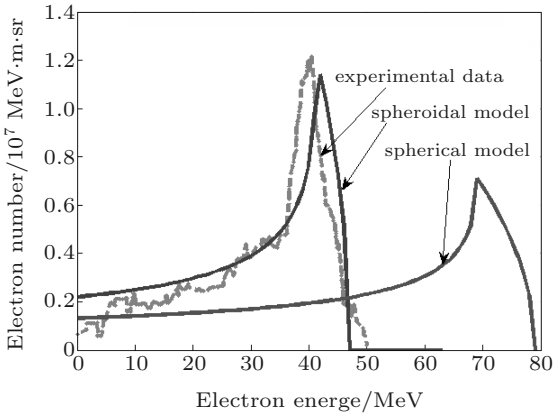


Fig. 2. Comparing the predicted electron energy distribution according to the earlier spherical regime and here-mentioned spheroidal models with the experimental data. The maximum energy of the spheroidal model is less than the spherical model and closer to the experimental data.

5. Conclusion

In the present work, we derived analytical expressions for the potential within a cavity moving at relativistic velocity in plasma. We improved the previous models by appropriately handling the bubble velocity approaching to the velocity of light and derived the spheroidal potential. We derived the maximum energy of electrons and we showed that the maximum energy of spheroidal model is less than the spherical model.

The electron energy spectrum is also obtained and it is found that the energy distribution ratio of electrons ($\Delta E/E$) for the spheroidal model under the conditions reported here is half that of the spherical model and it is in good agreement with the experimental value under the same conditions.

Acknowledgment

Project supported by the Research Deputy Office in the Islamic Azad University of Maragheh Branch.

References

[1] Tajima T and Dawson J M 1979 *Phys. Rev. Lett.* **43** 267
[2] Chen P, Dawson J M, Haff R W and Katsouleas T 1985 *Phys. Rev. Lett.* **54** 693
[3] Chen P, Dawson J M, Haff R W and Katsouleas T 1985 *Phys. Rev. Lett.* **55** 1537
[4] Pukhov A and Meyer-ter-Vehn J 2002 *Appl. Phys.* B: *Lasers Opt.* **74** 355
[5] Kostykov I, Pukhov A and Kiselev S 2004 *Phys. Plasmas* **11** 5256
[6] Lifschitz A F, Faure J, Glinec Y, Malka V and Mora P 2006 *Laser Particle Beams* **24** 255
[7] Mangles S P D, Thomas A G R, Lundh O, Lindau F, Kaluza M C, Persson A, Wahlström C G, Krushelnick K and Najmudin Z 2007 *Phys. Plasmas* **14** 056702
[8] Hidding B, Amthor K U, Liesfeld B, Schwoerer H, Karsch S and Geissler M 2006 *Phys. Rev. Lett.* **96** 105004
[9] Mangles S P D, Murphy C D, Najmudin Z, Thomas A G R, Collier J L, Dangor A E, Divall E J, Foster P S, Gallacher J G, Hooker C J, Jaroszynski D A, Langley A J, Mori W B, Norreys P A, Tsung F S, Viskup R, Walton B R and Krushelnick K 2004 *Nature* **431** 535
[10] R C G, Geddes, Toth Cs, van Tilborg J, Esarey E H, Schroeder C B, Bruhwiler D, Nieter C, Cary J and Leemans W P 2004 *Nature* **431** 538
[11] Faure J, Glinec Y, Pukhov A, Kiselev S, Gordienko S, Lefebvre E, Rousseau J P, Burgy F and Malka V 2004 *Nature* **431** 541
[12] Sadighi-Bonabi R, Rahmatallahpor S, Navid H A, Lotfi E, Zobdeh P, Reiazie Z, Bostan M D and Mohamadian M 2009 *Contrib. Plasma Phys.* **49** 49
[13] Zobdeh P, Sadighi-Bonabi R and Afarideh H 2008 *Plasma Devices and Operations* **16** 105
[14] Zobdeh P, Sadighi-Bonabi R and Afarideh H 2009 *Physics of Particles and Nuclear Letters* **6** 419
[15] Sadighi-Bonabi R, Navid H A and Zobdeh P 2009 *Laser Particle Beams* **27** 223
[16] Halliday, Resnick, Walker: *Fundamentals of Physics*, 6th edn. (New York: John Wiley & Sons)
[17] Esirkepov T, Bulanov S V, Yamagiwa M and Tajima T 2006 *Phys. Rev. Lett.* **96** 014803